N91-25994

DEIMOS: A FEATURELESS ASTEROID-LIKE SPECTRUM; W. M. Grundy and U. Fink, Lunar and Planetary Laboratory, University of Arizona, Tucson, AZ 85721.

We obtained high quality CCD spectra of Deimos from 0.5 to 1.0 μm at a spectral resolution of 15 Å at the time of the 1988 Mars opposition. Our data acquisition and reduction methods allowed us to quantitatively prevent scattered light from Mars from contaminating the spectra. Solar analog stars BS560, BS2007, and BS8931 were observed the same night to allow removal of telluric absorptions. The ratio spectrum of Deimos has a red slope, increasing in reflectance by a factor of ~50% over the one-octave wavelength interval observed. Other than this slope, the spectrum is remarkably featureless. The absence of absorption bands in the spectrum of Deimos is in marked contrast with the spectra of Martian surface materials. No trace of the Fe^{2+} charge transfer absorption band around 1 μm is observed, which rules out the presence of significant quantities of minerals such as the pyroxenes or olivines at the surface of Deimos. The featureless red spectrum of Deimos appears to be consistent with a surface composition of fine grained carbonaceous chondrite type material. We will present an analysis of the spectrum of Deimos which makes use of the Hapke scattering surface model.

This work was supported by NASA grants NAGW 1549 and NGT 50661.

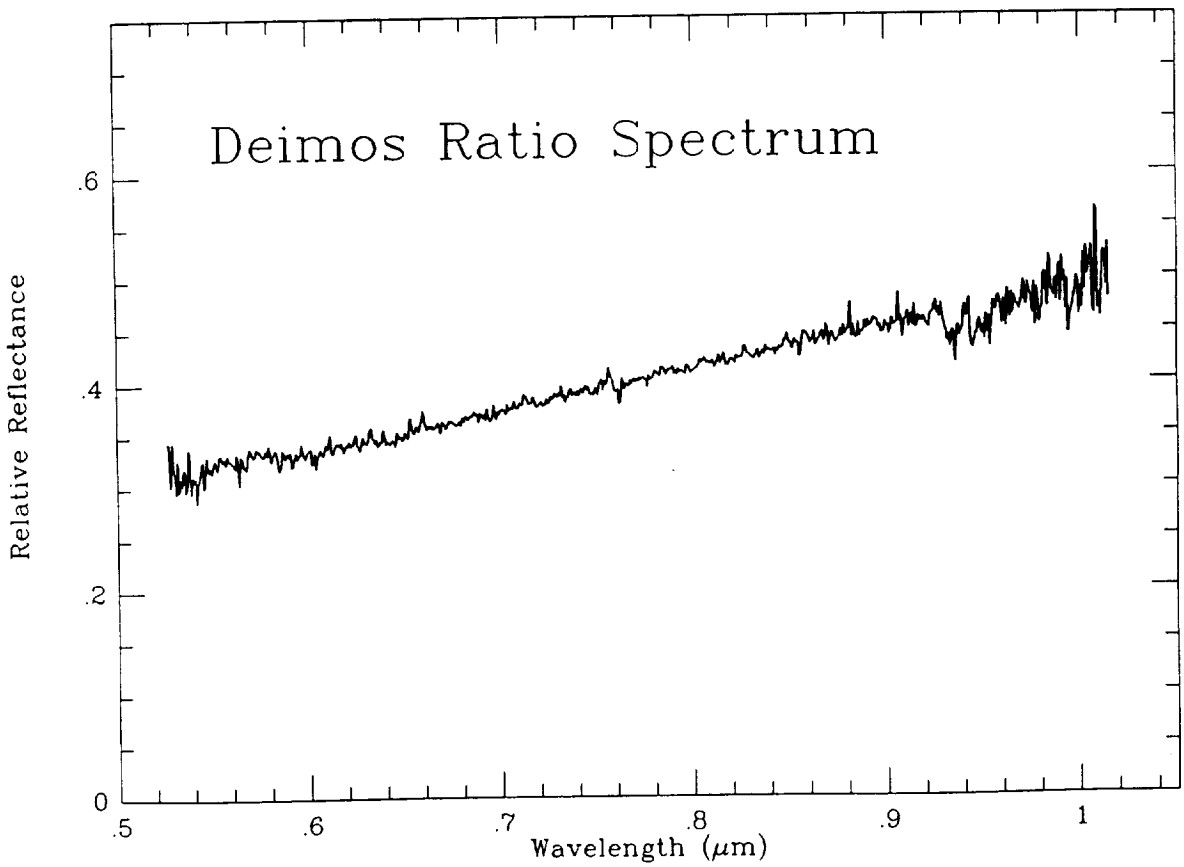

ON THE COMMON GENETIC CONNECTION AND MUTUAL CONDITIONALITY OF THE FORMING OF STABLE STRUCTURES IN CENTRAL GRAVITATING SYSTEMS

Yu.K.Gulak
Pedagogical Institute, 314000 Poltava, USSR

1) Mathematical uniformity of gravitational interaction in planetary systems (PS) of Sun, solitary planets, its massive satellites (S);

2) non-zero central bodies (CB) sizes $r_0 \neq 0$ and mutual restriction $r_g \neq \infty$ of each PS $\Delta r = r_g - r_0$;

3) the in force field of CB energy and angular momentum conservation laws, those are obligatory for every S, which mutually perturb their radial, azimuthal, and latitudal components of motion;

4) sufficiently large number of different masses (fractions) in the system;

5) the natural selection of the permanent S and their separation into the fractions (into degrees of pliability to mutual perturbations), i.e. relaxation, transition to stable state of spatially limited oscillating systems with many degrees of freedom;

6) these obvious from a classical physics' positions theses

a) secure a structuring of PS: forming within them "continuous-discrete" radial, azimuthal, and latitudal standing waves in superposition of which every satellites introduces its own deposit as a bearer of its spatial continuous force field. Such waves really exist and show (is observed) in PS as a system of mutually limiting and shepherding rings (belts), along which move these separated fractions of S. Analogous by nature waves are reproduced easy in laboratory tests;

b) permit to obtain the equation, which is mathematically identical with Schrödinger equation, but (in contrast to the latter) to have physically clear in classical physics' spirit interpretation of each from membering functions, values, and obtained solutions. The direct connection between a CB mass and constant, which takes the place of Planck's constant, is determinad theoretically. Here a misterious nature of this constant as well as connected with it quantum phenomena also acquire a sense of the wellknown images of classical physics: in particular the mathematical "density waves of probability", quantum regularities of radiation and absorption, spin phenomena etc..

Thus, genetic unity of structural formating in the large and small bodies-satellites medium is determined in cosmic planetary systems. It is difficult not to conclude in this a deep analogy between the mechanics of the cosmic and atomic systems, if one remembers the mathematical closeness of the laws of Newton and Coulomb.

REGULARITIES OF THE ORBITAL DISTRIBUTION OF ASTEROIDS, COMETS AND METEORS

Yu.K.Gulak, I.A.Dichko
Gravimetric Observatory of Ukrainian Acad.Sc.314000 Poltava,USSR

Regularities of the orbits of gravitating matter's radial distribution in the Solar system (planets, asteroids, comets, and meteoric bodies, satellites and meteoric matter in planetary systems) are discussed in this report. The orbits of the bodies-satellites tend to group themselves in commensurable (quantum) distances from the attractive centre according to the proposed theory (see report by Gulak), so that their semi-major axes a_n may be shown by an all common gravitational systems formula: $a_n = n a_o/2$, where: n- natural series number, a_o- commensurability element, which is determined singly by the central body mass M of the system: $a_o = \beta M^{7/9}$. Empiric determination of the integration constant β showed, that it doesn't differ practically within a huge range(which exceeds seven powers of ten) of the values M in the Solar system.

Mean semi-major axes within annular systems of asteroids clearly separated by gaps conform well to theoretical calculations using the above formula. 26 orbits between Mars and Jupiter were predicted in 1959 using this theory. In 1959 only 6 of these orbits were found to be occupied by asteroids. In 1969, in connection with the discovery of new asteroids, 8 more of the 26 orbits were found to be occupied, and in 1979 9 more of the original 26 were found to be occupied, leaving 3 orbits yet to be verified.

As regards to comets nuclei (cometoids) then the works by E.I.Kazimirchak-Polonskaya and Yu.K.Gulak showed that they have a property to be in a stable condition based on the pre-calculated orbits of our theory. It is implied in favour with this that whole comet body belts (which are sorces of short-period comets) may be there between giant planets, not only in Oort cloud.

Graundbased observations and calculations of the hundreds of thousands of meteoric bodies' orbits show that its distribution is "formed under the potent influence of macroquantum phenomena" (Yu.I.Voloshchuk, B.L.Kashcheev). These authors draw a conclusion that Gulak's theory gives the best correspondence under comparison of cited observations with the theories by Gulak, Quiroga and Chechelnicky.

The planetary rings including the recently discovered Uranian and Neptunian rings give a good correspondence with this theory, as well as dusty belts around the Earth and Moon (spacecrafts Electron 1-3, Geos-2, Luna-10, Pioneer-9, 10).

The report is illustrated by the tables of gravitating matter's distributions in the systems of Sun, Earth, Jupiter, Saturn, Uranus, and Neptune.

THE SHAPE OF METEOR STREAMS IN ORBITAL PARAMETER SPACE FROM INDEPENDENT METEOR SURVEYS.

B.Å.S. Gustafson

Astronomy Department, University of Florida 211 SSRB, 32611 Florida, USA.

A measure of meteoroid number density based on Drummond's (1981, *Icarus* **47**, p. 545-553) measure of orbital similarity is used to chart the meteoric complex and the extent of major meteor streams in orbital parameter space. Bias correction reveals both narrow congregations and extended structures that may be related to streams. The measure of meteoroid number density can help discriminate between meteor streams. The Tisserand quantity and a set of other "quasi-stationary parameters" were tested on actual meteor streams as an additional discriminant.

SIZE DISTRIBUTION DEPENDANCE OF INFRARED EMISSION FROM MODELS OF ASTEROIDAL AND COMETARY DUST.

B.Å.S. Gustafson

Astronomy Department, University of Florida 211 SSRB, 32611 Florida, USA

Emission efficiencies from near-infrared to far-infrared wavelengths are calculated for two models of asteroid comminute particles and compared with those for a model of cometary dust. The asteroid dust models have higher efficiencies than the cometary dust model of dimensions smaller than the wavelength; but the comet dust model produces more thermal radiation per unit mass. Particles smaller than 10 μm in size dominate the brightness from asteroid dust in the collisional equilibrium size distribution. However, particles in the 10 to 100 μm size range dominate in populations of the cometary and asteroidal dust when the empirical interplanetary size distribution by Grün *et al.* (1985, *Icarus,* **62,** p. 244-272) is applied. While the temperatures of large cometary and asteroidal particles of all concave shapes are within approximately 6% of the black-body equilibrium temperature, the temperatures of the brightest particles deviate substantially from that of a black-body. Cometary dust appear hotter, while asteroid produced dust may appear colder depending on the size distribution below 100μm.

MODELLING OF LONG TERM EVOLUTION AND EQUILIBRIUM STATE OF A DUST COMPONENT FROM THE ASTEROID BELT

B.Å.S. Gustafson[1], E. Grün[2]

1) Astronomy Department, University of Florida 211 SSRB, 32611 Florida, USA.
2) Max-Planck Institut für Kernphysik, Postfach 10 39 80, D-6900 Heidelberg 1, FRG.

The size distribution of collisional debris from an asteroid in the main belt is modeled over time periods of millions of years. The dust is allowed to collide with a background population of dust and meteoroids as they spiral toward the Sun under the action of Poynting-Robertson drag. The background population is modelled using the empirical interplanetary size distribution by Grün *et al.* (1985, *Icarus,* **62,** p. 244-272). The resulting time dependent size distribution at 1 AU is presented along with the heliocentric particle number density distribution as a function of particle mass. As an equilibrium state is approached, deviations from the equilibrium size distribution based on "particles in a box" -model is described.

A SEARCH FOR STREAMS ASSOCIATED WITH EARTH-APPROACHING ASTEROIDS 3551, 3908, AND 4055.

B.Å.S. Gustafson[1] and I.P. Williams[2]

1) Astronomy Department, University of Florida 211 SSRB, 32611 Florida, USA.
2) School of Mathematical Sciences, Queen Mary and Westfield College, University of London, Mile End Road, London E1 4NS, England.

Based on spectral similarity Cruikshank *et al.* (1991, *Icarus* **89,** p. 1-13) suggested that a set of basaltic Earth-approaching asteroids (3551, 3908, 4055, and possibly Vesta) are fragments produced in a collision that may also have generated a stream of basaltic meteoroids. They argue that the stream might be producing Eucrites, Howardites, and Diogenites (HED meteorites) with similar spectra.

This article presents a search for meteor orbits near these asteroids in twelve independent photographic and RADAR surveys. A procedure to search for streams in a wider range of orbital parameter space is presented and used on the 1968-1969 synoptic year Harvard RADAR survey (Sekanina and Southworth, 1975, NASA CR-2615) and graphically reduced Super Schmidt orbits (McCrosky and Posen, 1961, *Smithsonian Contr. Astrophys.*, **4,** No.2). The relatively small set of graphically reduced fireball orbits by McCrosky *et al.* (1976, *Meteoritica,* **37,** p.44-59) are also searched, as the survey was specifically aimed at detecting meteorite dropping fireballs. These survey's were corrected for some of their bias and an attempt made to judge the significance of the meteor associations.

LIGHT SCATTERING BY OPEN-STRUCTURED, FILAMENTARY, COMET DUST MODELS

B.Å.S. Gustafson[1], R.H. Zerull[2], K. Schulz[2] and E. Corbach[2]

1) Astronomy Department, University of Florida 211 SSRB, 32611 Florida, USA.
2) Ruhr-Universität, Fakultät für Physik und Astronomie, Bochum, F.R.G.

A simulation experiment of the light scattering by comet dust was performed at the microwave analogue scattering facility of the Ruhr-Universität Bochum in the Federal Republic of Germany. The scattering targets are designed to approximate the morphology of cosmic dust including cometary and nebular dust. The models can be described as open-structured aggregates of submicron silicate spheres with or without an absorbing mantle. Whether the models are fractal or not is a matter of terminology. They encompass a range of fractal dimensions near 1 to approximately 3. Efficiency factors for extinction, absorption, scattering and radiation pressure will be presented. The angular dependence of scattered intensity and polarization is also shown.

LONG-TERM EVOLUTION OF 1991 DA: A DYNAMICALLY EVOLVED EXTINCT HALLEY-TYPE COMET? G. Hahn & M.E. Bailey, Department of Astronomy, The University, Manchester M13 9PL, England, U.K.

The long-term dynamical evolution of the recently discovered intermediate-period asteroid 1991 DA and a bundle of similar orbits has been followed for $\pm 100,000$ years in a model solar system including the Earth through Neptune. The orbit of 1991 DA is close to the 2:7 resonance with Jupiter; it avoids close encounters ($\Delta < 1$ AU) for at least the past 30,000 years even at the node crossing. This is due to libration of the critical argument σ. Apart from small perturbations due to close encounters with Mars and Uranus in the recent past ($t \simeq -2000$ yr), the orbit evolves mainly through perturbations by Saturn; the time between node crossings with Jupiter or Saturn is $\approx 3 \times 10^4$ yr. Strong secular evolution about 5×10^4 yr ago causes changes in the perihelion distance to $q < 1$ AU and large-amplitude variations in the eccentricity and inclination ($25° \lesssim i \lesssim 75°$). These are similar, for example, to those found in P/Machholz. The long-term orbital evolution of 1991 DA is illustrated, while the connexion between high-inclination, intermediate-period, small q orbits and those of observed Halley-type comets is emphasized. If 1991 DA was indeed a comet, it is not surprising that it is now extinct; searches for residual, low-level cometary activity and associated dust streams should be encouraged.

Dynamical Constraints on Material Orbiting Asteroids

D. P. Hamilton and J. A. Burns (Cornell University)

As Galileo's Gaspra flyby draws near, questions of the quantity and spatial distribution of material which might be found in its vicinity become critically importance to spacecraft mission planners who are making final decisions on how closely to approach this small asteroid. Obviously, in the absence of any perturbations, particles can move on Keplerian orbits at any distance from an asteroid. In reality, however, gravitational perturbations from the Sun and planets, and solar radiation pressure will limit the zone in which particles can stably orbit. Following many other studies, we discuss elsewhere (Hamilton and Burns, Icarus in press) the size and three-dimensional shape of the stability zone for an asteroid that moves along a circular heliocentric orbit, ignoring solar radiation pressure and perturbations from Jupiter. We find that the stability zone scales like the radius of Hill's sphere and that orbits are stable out to lesser distances over the orbital pole than in the asteroid's orbital plane. Chauvineau and Mignard (Icarus 1990, 87, 377) consider how Jupiter perturbs planar orbits about the asteroid and show that the consequent diffusion of the Jacobi constant leads to additional escapes. Here we discuss two further perturbation effects: the influence of the asteroid's orbital eccentricity and the contribution of solar radiation pressure.

We find numerically that the relatively large eccentricity of Galileo's target Gaspra significantly reduces the size of the stability zone for test particles that are followed for five orbits of the asteroid around the Sun. The figure shows the maximum height (measured in asteroid radii) attained for a series of test cases as a function of initial inclination off the asteroid's orbital plane. The solid circles are for an asteroid moving on a circular orbit and the crosses are for one with Gaspra's eccentricity (e=0.17). We see that orbits around an asteroid with sizable eccentricity rise to lesser heights than those around an asteroid with zero eccentricity.

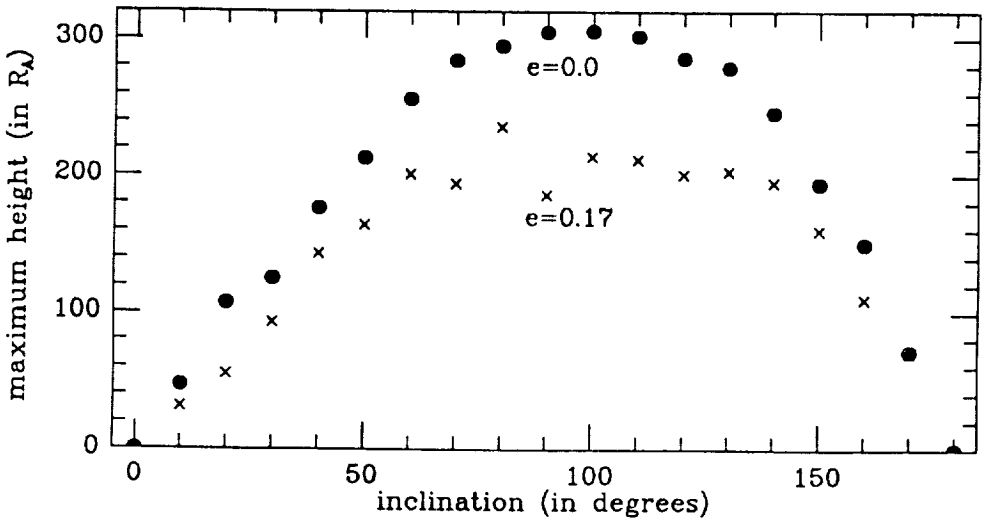

Radiation pressure is found to be surprisingly effective in removing mm and cm sized particles from circum-asteroidal orbits. For such large particles in orbit around the Sun or the planets, radiation pressure can be safely ignored, but in the shallow gravitational well of an asteroid it is a strong perturbation. We find that particles satisfying the following inequality are forced to crash into the asteroid:

$$s(cm) < 1.7\left(\frac{r(km)}{1000}\right)\left(\frac{2.2}{a(AU)}\right)\left(\frac{M_{Gaspra}}{M_{Asteroid}}\right)\left(\frac{Q_{pr}}{1.0}\right)\left(\frac{2.5}{\rho(g/cm^3)}\right);$$

these collisions occur in timescales shorter than the asteroid's orbital period. Here s is the particle's radius, r is its distance from the asteroid, a is the asteroid's distance from the Sun, the M's are masses, Q_{pr} is a radiation efficiency coefficient with an expected value near unity and ρ is the particle's density. Coincidentally, a size distribution consisting of solely mm and cm sized particles is the most dangerous to a spacecraft for a given amount of mass in orbit around the asteroid. Combining observational constraints on the optical depth with the changes in the size distribution from orbital evolution induced by radiation pressure, the worst-case probability for a crippling collision should be reduced.

HIGH PRECISION PHASE RELATIONS OF DARK, LIGHT, AND INTERMEDIATE ASTEROIDS

A.W. Harris, Jet Propulsion Laboratory

A fundamental hypothesis in the formulation of the H-G magnitude system is that all phase curves can be represented as a linear combination (in intensity space) of two phase curves. The physical motivation is the assumption that the singly scattered and multiply scattered components have the same phase dependance for any surface; thus the resultant phase curve is a linear sum of the two components, with the ratio of each loosely related to the albedo of the surface. To test this hypothesis, it is not necessary to "observe" the pure single-scattered and multiple-scattered phase relations. Any two phase relations, sufficiently different from one another, should be able to match any other phase relation as a linear combination (in intensity space) of the first two. A simple corollary is that if any two phase curves (normalized at zero phase angle) cross over at another phase angle, then all phase curves must pass through that point. In the figure below, we present three high precision phase curves: 44 Nysa, one of the highest albedo asteroids known (These data are from Harris, et al., Icarus 81, 365-374, 1989); 47 Aglaja, a moderately dark C Class asteroid (Harris, et al., this conference); and 113 Amalthea (previously unpublished data). Amalthea is higher than average albedo, but about intermediate between 44 and 47. All three curves have been adjusted to the same level at zero phase angle. Each curve crosses over the other two, none at the same phase angle, thus violating the above stated corollary. (The corollary applies in either magnitude or intensity space.) Thus it is clear that the fundamental postulate of the H-G system is not valid, and a more complete theory must be sought.

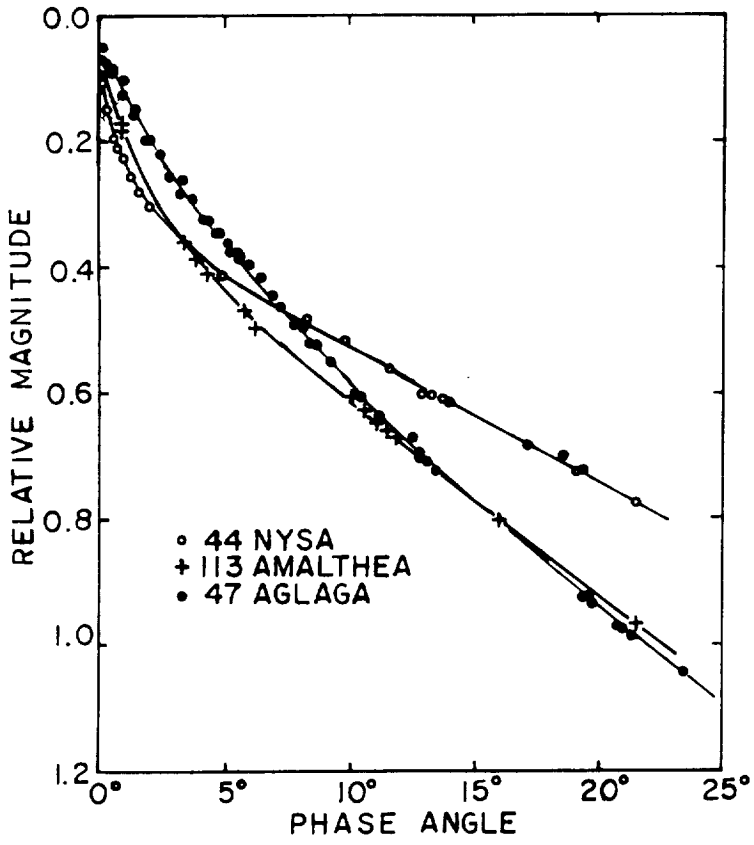

PHOTOELECTRIC LIGHTCURVE AND PHASE RELATION OF 47 AGLAJA

A.W. Harris, G.P. Chernova, D.F. Lupishko, J.W. Young, N.N. Kiselev, L.V. Jones, and B.J. Wallace

Millis, et al. (Icarus 81, 375-385, 1989) present occultation and photometric results for 47 Aglaja which indicate that it is a fairly dark asteroid (albedo = 0.071 on the H-G system). The phase curve presented shows considerable variation in intrinsic brightness with different aspects, but coverage at any one opposition was insufficient to fully define G, and allow accurate assessment of the relative light levels each year. Furthermore, there was some indication that Aglaja might be substantially deficient in opposition effect with respect to the H-G model, as had been found for several other dark asteroids (cf., Harris and Young, Icarus 81, 314-364, 1989). We embarked on an international observing campaign in 1989 in order to resolve some of these issues. The resulting data set, from 4 observatories in the USSR, USA, and Columbia, is the largest data set ever obtained on a single asteroid at one apparition, consisting of over 2000 individual observations on about 50 nights. The period was determined unambiguously, P = 13.176 ±0.001 hours, and the phase curve was sampled thoroughly from phase angle 23° down to 0°.10. The phase relation is indeed less curved (less opposition effect) than predicted by the H-G model. By drawing a smooth curve through the phase data, and assuming the same curve at other oppositions, it was possible to define the relative light levels at 5 other observed apparitions. These results confirm the conclusion of Millis, et al. (1989) that Aglaja was observed nearly pole-on in 1979, at ecliptic longitude 330°.

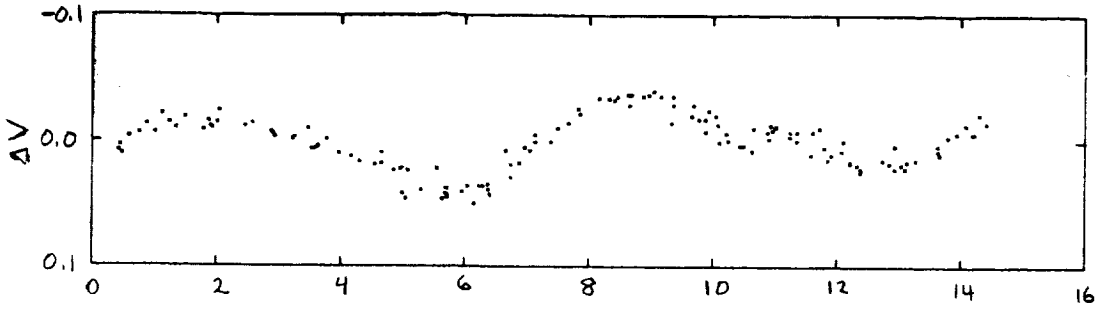

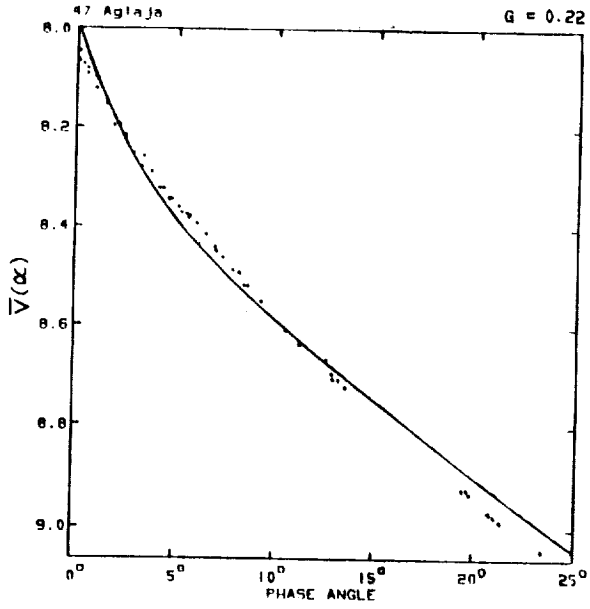

The data used in the composite lightcurve (above) have been heavily averaged to reduce clutter of plotted points. The vertical scale is 0.1 mag. per tick, and the horizontal scale is 2 hr per tick. The phase plot (left) shows the deviation of the best-fit H-G relation (solid line) from the observed phase relation (dots).

A CORVID METEOR SHOWER IS PREDICTED FOR 2003 OR 2006

Jack B. Hartung, Max-Planck-Institute für Kernphysik, 6900 Heidelberg, Germany.

The Corvid meteor stream was observed only once, from June 25 to July 2 in 1937. Its observed radiant is given by a right ascension of 192° and a declination of -19°. The direction of motion of Corvid meteoroids, which is just opposite to their radiant, is given by a right ascension of 12° (192° - 180°) and declination of +19°.

The formation of the lunar crater, Giordano Bruno (GB), was observed on the evening of June 25, 1178 (Gregorian calendar). On that evening the phase of the Moon was 19.5° past new moon, the ecliptic longitude of the Sun was 93°, and the optical libration in longitude was 1.5°. The location of GB is lunar latitude, 36° N., and lunar longitude, 103° E. With these data one can determine the ecliptic longitudes of the lunar prime meridian, 294° (93° + 19.5° + 1.5° + 180°), and the zenith direction at GB, 37° (294° + 103° - 360°). The ecliptic latitude of the zenith direction is approximately +36°. By transforming from ecliptic to equatorial coordinates we obtain the right ascension, 18°, and declination, 47°, of the zenith direction at GB at the time of the impact.

By solving a spherical triangle we find the angle between the zenith direction at GB and the direction of motion of Corvid meteoroids to be 28°. Laboratory experiments show that for ejection velocities of 2.4 km/sec, the lunar escape velocity, the angle between the ejecta direction and the local vertical (zenith) is also 28°! It seems beyond coincidence that the observed direction of motion of Corvid meteoroids and one independently expected direction of ejecta motion based on experiments are identical.

If ejecta from the GB impact is to be seen in late June many years later at the Earth, an integer number of ejecta orbits must be executed during exactly the time required for the Earth-Moon system to complete an integer number of orbits. The year of the GB impact, 1178, differs from the only year Corvid meteors were observed, 1937, by 759 years. If a connection between these two events exists, then 759 must be the product of two integers, one representing the number of years, or Earth orbits, between Earth-Corvid encounters, and the second integer representing the number of such encounters that have occurred through 1937. Integer factors of 759 are: 3, 11, 23, 33, 69, and 253. The period of the Corvid orbit is limited to those numbers which, when divided into any of these factors, yield integer quotients, the integer quotients representing the number of Corvid orbits between each Earth-Corvid encounter. Therefore, for each integer factor we can state unequivocally which years could yield observable Corvid meteors.

Factors 3 and 11 can probably be ruled out because encounters would be expected every 3 or 11 years, respectively. Encounters so often should have been observed, although 1992 (1937 + (5 x 11)) should not be ignored. It is possible that appropriate observations were not made in late June of 1948, 1959, 1970, or 1981. The next possible opportunity to observe Corvid meteoroids, if they were, in fact, produced by the GB impact in 1178, will be in late June of 2003 (1937 + (2 x 33)). Another opportunity will occur in 2006 (1937 + (3 x 23)). Accordingly, I predict that another Corvid meteor shower will occur in late June and early July of 2003 or 2006.

LIGHTCURVE OF COMET AUSTIN(1989C1) AND ITS DUST MANTLE DEVELOPMENT; H. Hasegawa, ASTEC, Inc. and J. Watanabe, National Astronomical Observatory

Brightness variation of comet Austin(1989c1) was investigated in terms of the variations of water production rate. We used Newburn's semi-empirical law to translate the visual brightness data into water production rates. The curve of the water production rates as a function of heliocentric distance was compared with the model calculations that were assumed energy balance between solar incident and vaporization of water. Thermal flow in a dust mantle at a surface of the nucleus is also included in the model. The model calculations including the dust mantle are more favorable to the observed rate than the non-dust mantle cases. It is also expected that the dust mantle would have been developed when the comet was at a large heliocentric distance before the perihelion passage. Dust tail analysis of the comet showed such dust release. And the extinction after the perihelion passage suggests that the dust mantle was developed gradually.

COMET CHARACTERISATION AND LANDING: STATUS OF ESA STUDIES FOR ROSETTA

M. Hechler, J. de Lafontaine
European Space Agency

The Rosetta mission, one of the cornerstones of the ESA Space Science programme, has the objective of returning a comet nucleus sample to Earth laboratories, preserving its fundamental chemical and physical properties. It is believed that the analysis of cometary material will provide answers to questions related to the origin and early evolution of the solar system. The mission design and the spacecraft system have been studied jointly by NASA and ESA. A description of the baseline mission scenario is presented by A. Atzei and R. Mitchell at this Conference. In parallel to the mission definition activities, a series of technology studies sponsored by ESA have been addressing the critical elements of the mission which are mainly related to its near-comet phases. An overview of the current Rosetta mission planning in the near-comet phases before landing is presented here, as it is currently foreseen in the studies carried out within ESA and in Industry under ESA sponsorship.

The near-comet phases until landing include: (1) the Approach Phase, (2) the Observation Phase, and (3) the Descent and Landing Phase. The Approach Phase begins with comet acquisition by the on-board camera. With a sequence of orbital manoeuvres commanded from the ground, the spacecraft velocity is progressively reduced. For safety, the spacecraft trajectory is never directed at the comet but the fly-by distance is also gradually decreased to perform an orbital rendez-vous with the comet, a few hundreds of kilometers above it. During the approach, a preliminary identification of the comet kinematic and geometrical characteristics is obtained, using ground processing of on-board and ground-based observables.

After entering the gravitational field of the comet (some 30 to 1300 km above it, depending on the comet mass), the spacecraft acquires a succession of remote-sensing orbits around the nucleus. The Observation Phase activities begin with a global mapping of the illuminated part of the comet. Near-circular polar orbits are selected to maximize the coverage while satisfying the requirements of constant communication link with the ground stations. Based on these data, three to five candidate landing sites are selected by the ground and subsequently analyzed in more detail from eccentric orbits which overfly these locations at about 5 km altitude. Detailed maps of the candidate landing areas (500 m x 500 m) in the visible, the infrared and the thermal infrared spectra are acquired to determine their suitability from safety and scientific interest points of view. The site safety assessment is also supported by a laser ranging instrument that provides a detailed topographic map of the area in terms of altitude profiles. In addition, subsurface radar sounding may support the landing site selection. During the observation activities, on-board measurements and tracking data from ground are processed to estimate the comet kinematics, its gravitational field and the spacecraft orbit to an accuracy required for the safe navigation and guidance of the spacecraft to the desired landing point. Once these parameters are uplinked from ground, the autonomous Descent and Landing Phase towards the selected landing site is initiated from an approach orbit at a few kilometers above the surface.

Two descent scenarios, a primary and a back-up, are foreseen for the Rosetta mission. In the nominal case, the spacecraft autonomous navigation relies on the laser range finder. Elevation maps are built in real time with the scanning instrument and are compared with on-board maps stored earlier, at the end of the Observation Phase. Accurate information on the spacecraft horizontal position are thus derived. In the alternate case where the laser may have failed, the spacecraft horizontal position is predicted by on-board models but a microwave radar ensures landing safety by searching and locking on a detected flat area. In both scenarios, precise altitude, velocity and attitude measurements are available from the radar system. Numerical simulations have demonstrated that landing accuracies of the order of 20 m in the baseline scenario and 200 m in the second one (3 sigmas) can be achieved.

Further refinements to these strategies are currently being performed in the ESA studies. More detailed analyses are also conducted to design and test the ground-based and on-board algorithms required for spacecraft navigation, guidance and control. Microprocessor implementation of some of the on-board algorithms is foreseen by the end of 1992.